

---

# Using point cloud comparisons for revealing deformations of natural and artificial objects

Christoph HOLST, Lasse KLINGBEIL, Felix ESSER, Heiner KUHLMANN

University of Bonn, Institute of Geodesy and Geoinformation  
Bonn, Germany  
E-mail: c.holst@igg.uni-bonn.de

## Abstract

For the sampling of natural and artificial objects with high spatial resolution, terrestrial laser scanners (TLS) or cameras, e.g., mounted on unmanned aerial vehicles (UAV), are often used. Both sensor measurements either directly lead to a point cloud or a point cloud can be derived by several photogrammetry based processing steps. If measured in several time epochs, the point clouds can reveal areal deformations of the sampled objects. For this, point cloud comparisons (i.e., mesh-to-mesh, M2M, and multiscale-model-to-model-cloud comparison, M3C2) are frequently used since they aim at describing the geometric changes between two point clouds. The usefulness of these point clouds comparisons will be evaluated in this study based on TLS and UAV measurements of objects being subject to deformations, e.g., water dams, simple geometric bodies and solifluction lobes. It is revealed that the performance of point cloud comparisons in sense of describing the occurrence and magnitude of deformations strongly depends on the underlying type of deformation – rigid body movement or shape deformation – and on the deformation’s direction: in-plane or out-of-plane regarding the object’s and background’s geometry.

**Key words:** terrestrial laser scanner (TLS), unmanned aerial vehicle (UAV), deformation analysis, point cloud, M3C2 comparison

## 1 INTRODUCTION

In the past, natural and artificial objects have been monitored based on point-wise measurement techniques, e.g., total stations or levels. Since several years, terrestrial laser scanners (TLS) and cameras mounted on unmanned aerial vehicles (UAV) are increasingly used for deformations analyses. With these instruments, the data processing changes: The monitored object is sampled nearly continuously in space. Consequently, the strategies for deformation analysis do not consist of the comparison of signalized individual points in two epochs as described in Heunecke et al. (2013). Instead, geometric modeling of each epoch is performed to account for the densely sampled but less accurate measurements. Only after this modeling, both epochs are compared (Holst and Kuhlmann 2016). Examples are the monitoring of dams, tunnels and radio telescopes (Neuner et al. 2016, Mukupa et al. 2016). Laser scanners sample the surface based on polar measurements directly leading to a 3D point cloud. Contrary, a camera provides 2D images as measurements. Only after sampling an object repeatedly from different positions and/or orientations and with a certain overlap in the

---

TS 7 – Terrestrial Laser Scanning

images, the data can be processed to a 3D point cloud using a bundle adjustment or similar algorithms. Hence, in both cases, 3D point clouds are the outcome of the object sampling.

In principle, the comparison of two point clouds is possible in five different deformation models (Ohlmann-Lauber and Schäfer, 2011). Herein, the mesh-to-mesh comparison (M2M) and the multiscale-model-to-model cloud comparison (M3C2) are included. For more details, see Wunderlich et al. (2016), Neuner et al. (2016) and Holst et al. (2017b).

In M2M comparisons, each point cloud is meshed firstly and, afterwards, the shortest distance is calculated between each triangle of the reference point cloud to the nearest – corresponding – triangle of the other epochs' point cloud. In M3C2 comparisons, the number of points of one epoch is reduced by building core points that should represent the geometry of their neighbourhood of size  $D$ . These core points are gained by filtering. The difference to the other point cloud is then calculated along each core point's normal vector regarding its neighbourhood  $d$ . Hence, two neighbourhoods of size  $D$  and  $d$  need to be specified for this point cloud comparison. For a more detailed explanation, see Barnhart and Crosby (2013).

In general, these point cloud comparison do not only give the magnitude of the differences between correspondences but also a sign for each difference. Therefore, the directions of the normal vectors of each triangle or each cylinder, respectively, are used. These directions are consistent for neighboured correspondences if the surface of the reference point cloud is continuous.

Both methods for point cloud comparison, i.e., M2M and M3C2 comparisons, have been used widely for deformation analyses (Neuner et al., 2016). However, dependent on the type of deformation – rigid body movement or shape deformation – and dependent on the direction of deformation – in-plane or out-of-plane – point cloud comparisons can lead to false interpretations and, hence, misleading deformation analyses (Holst et al., 2017a, b).

The aim of this study is to further investigate the usefulness of point cloud comparisons for revealing deformations, dependent on the type and direction of deformation. Therefore, point clouds are simulated with different deformations between two epochs. The resulting point cloud comparison is evaluated: Can the true deformation be revealed? These findings are transferred afterwards to a concrete water dam, several artificial test objects and geomorphological processes. Since the results of the M2M and the M3C2 lead to similar conclusions, only the results of the M3C2 are shown in each case.

## 2 ANALYZING SIMULATED DEFORMATIONS

Holst et al. (2017a) already showed that the significance of a point cloud comparison for revealing deformations strongly depends on the type of deformation (rigid body movement or shape deformation) as well as on the deformation's direction in relation to the extent of the measured object (out-of-plane or in-plane). The result was that out-of-plane shape deformations are detectable best while in-plane rigid body movements are more difficult.

This can be explained by Figs. 1-2: If the surface changes its shape in the out-of-plane direction, the points assumed to correspond between two epochs indeed represent the same part of the surface. Contrary, if the object moves in-plane between both epochs, scan points that are assumed to be corresponding might represent different parts of the scanned surface: this especially holds for parts of the surface that are flat without large curvature, see Fig. 2. Here, the differences between both epochs do not indicate a deformation of the surface since they are not larger than without any movement. In regions, where the surface is curved or edged instead, differences are visible very well. Hence, although the surface moves in whole,

the magnitudes of the point cloud differences vary noticeably. Consequently, this kind of rigid body movement is harder to detect.

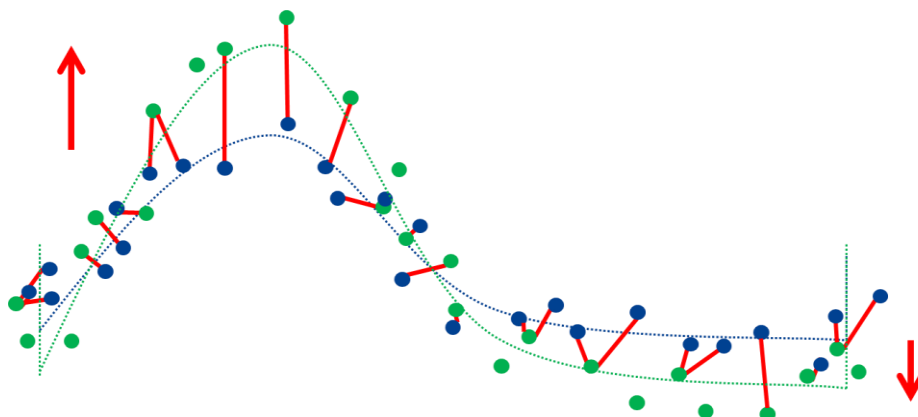


Fig. 1 Differences (red) between point clouds of epoch 1 (blue) and 2 (green) when a surface (blue/green dotted line) is deformed by an out-of-plane shape deformation

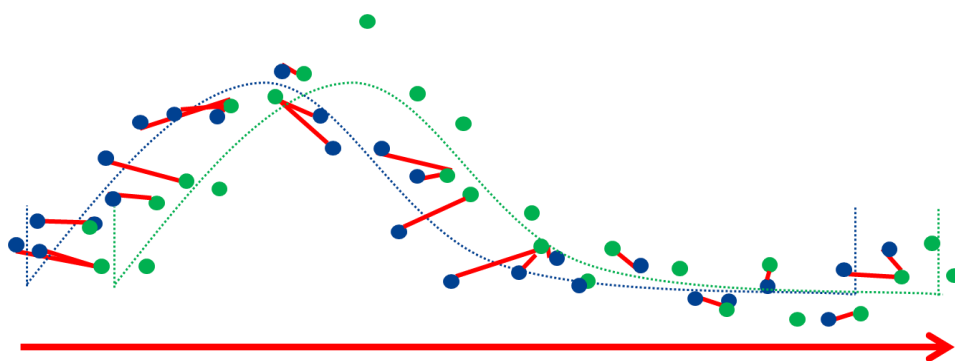


Fig. 2 Differences (red) between point clouds of epoch 1 (blue) and 2 (green) when a surface (blue/green dotted line) is deformed by an in-plane rigid body movement

These phenomena are studied further in subsequent simulations. The focus is led on the detection of rigid body movements (in-plane as well as out-of-plane) and additional out-of-plane shape deformations. Therefore, a 3D point cloud is generated based on scan points lying on a plane with a point spacing of 5 mm. Random errors of 2 mm standard deviation are added to every point. Additionally, an edged but planar object, i.e., a cuboid, and a smooth but curved object, i.e., a Gaussian distribution curve, are incorporated (Fig. 3). In the second epoch, these two objects either only move in-plane or their height grows additionally.

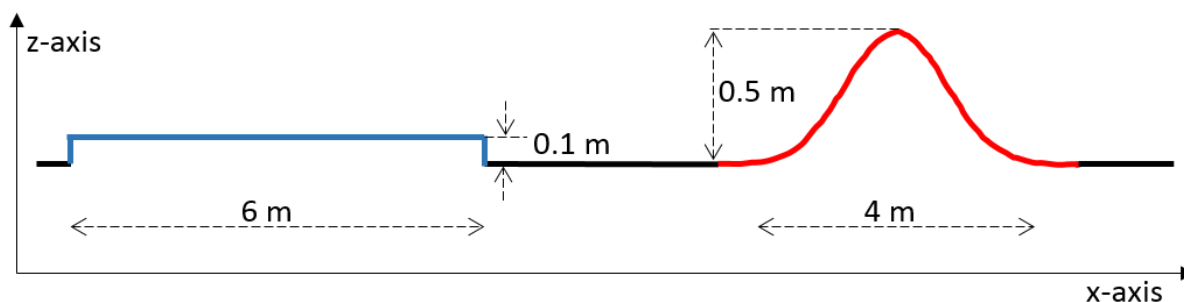
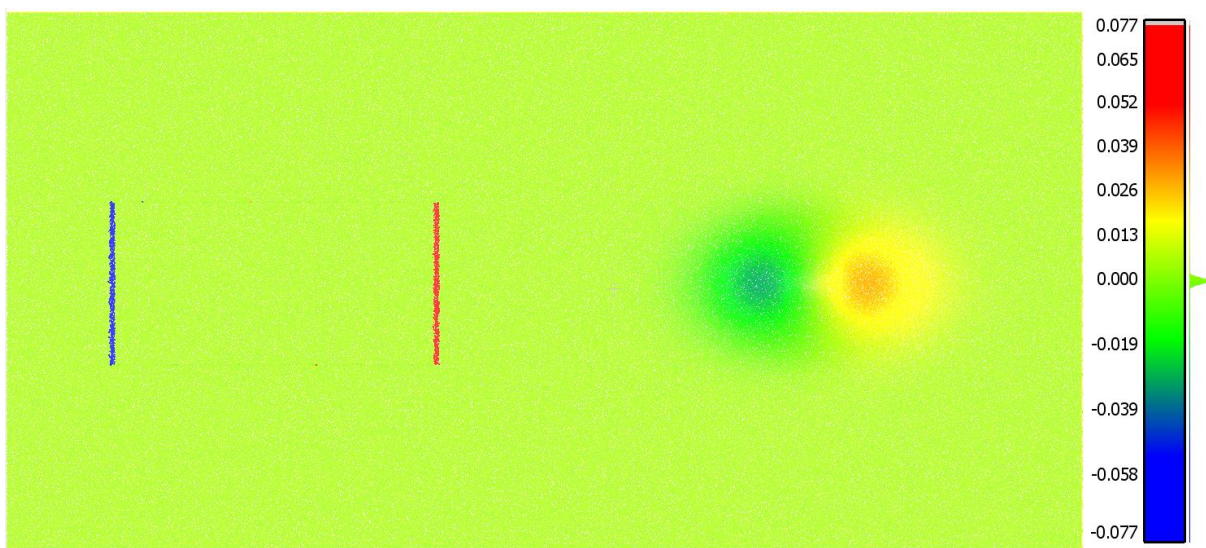


Fig. 3 Sketch of cross-section of simulated edged (blue) and curved (red) object (scaled between horizontal and vertical axis)

By performing a point cloud comparison between two epochs using the M3C2 approach, the results can be studied to identify patterns that indicate these specific deformations. As parameters,  $d = 50$  mm and  $D = 50$  mm are chosen. Hence, about  $10 \times 10$  neighbored points are used for defining the direction of each calculated difference as well as for defining the origin of the calculated difference in the reference point cloud.

## 2.1 IN-PLANE RIGID BODY MOVEMENT

An in-plane rigid body movement is simulated: both objects are moved along the x-axis for 100 mm. Fig. 4 shows the resulting point cloud comparison, using the M3C2 algorithm: the moved cuboid does only show larger differences at the edges, not at the planar parts. The magnitude of the differences at the edges equals about  $-75$  and  $+75$  mm. These values do not reflect the true movement of the object. Instead, the length along the x-axis of the regions showing this quantity equals about 100 mm. The reason for this is that the direction of the deformation is not the direction of the vector, which is the basis for the difference calculation. The direction of the vector depends on the parameters  $d$  and  $D$ : If these parameters were of other magnitude, the values of  $-75$  and  $+75$  mm would also change. Hence, the correspondences between the points in both epochs get lost.



*Fig. 4 M3C2 comparison of in-plane rigid body movement (CloudCompare)*

The movement of the Gaussian curve leads to a symmetric positive and negative smooth region of larger differences. The maximal differences are  $+25$  mm, the minimal ones  $-25$  mm. Again, these values do not correspond to the true movement due to the changed correspondences between the point clouds and due to the magnitudes of  $d$  and  $D$ . However, the symmetric appearance of the point cloud comparison can be remarked as a pattern for the in-plane movement of a smooth object.

Summarizing, an in-plane movement is hard to detect by a point cloud comparison. The magnitude of the differences does not indicate the true deformations in the presented example. Only the patterns of the deviations help in detecting a region, which has been deformed.

## 2.2 IN-PLANE RIGID BODY MOVEMENT TOGETHER WITH OUT-OF-PLANE SHAPE DEFORMATION

Now, the two objects are deformed by an out-of-plane shape deformation of 5, 10, 20 and 50 mm. Hence, they grow in direction of the z-axis as indicated in Fig. 3. The in-plane rigid body movement of 100 mm is applied at the same time. Fig. 5 shows the resulting point cloud comparisons from top (5 mm) to bottom (50 mm) for both objects.

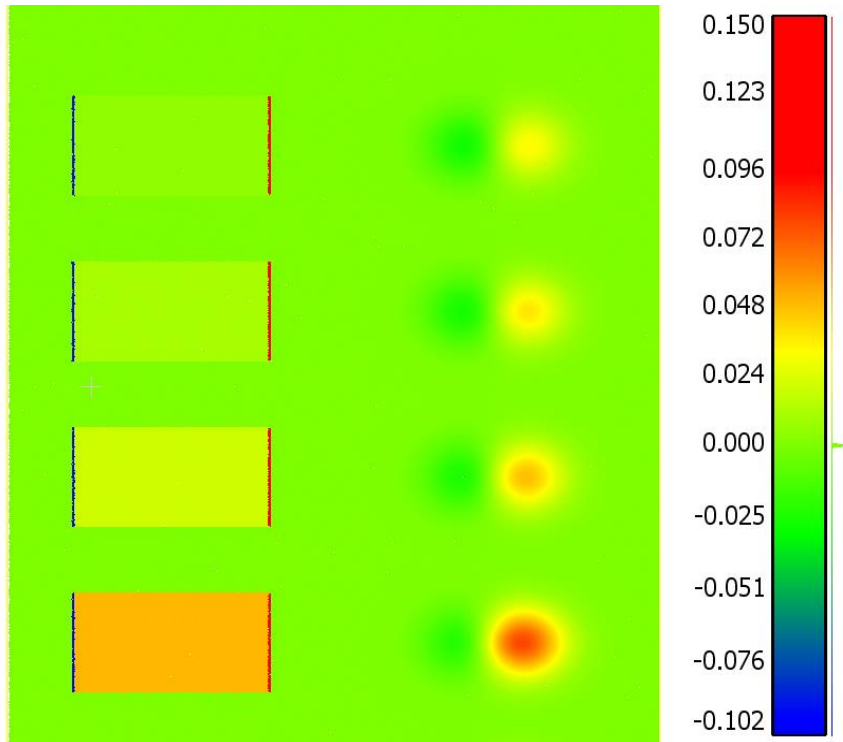


Fig. 5: M3C2 comparison for in-plane rigid body movement and out-of-plane shape deformation (CloudCompare)

For the cuboid, it can be stated: The results of an additional out-of-plane shape deformation of 5 mm are related to the ones without any shape deformation (see Fig. 4, notice different colorbar). Disagreements are identifiable at the planar surface of the cuboid that is also affected by larger differences. The larger the out-of-plane shape deformations get (from top to bottom in Fig. 5), the larger the point cloud differences on the planar surface of the cuboid get. The magnitudes of the differences on the planar surfaces are equal to the true shape deformation of 5, 10, 20 and 50 mm – disregarding the noise. The blue and red areas at the edges of the cuboids are unaffected by this increase.

For the Gaussian curve, the symmetry of the areas with negative and positive areas vanishes with increasing shape deformations. The positive differences grow up to +80 mm, the negative ones decrease in magnitude until about -20 mm.

Consequently, for the cuboid as well as the Gaussian curve, the effect of an additional out-of-plane shape deformation leads to different patterns in the point cloud comparison, compared to an exclusive in-plane rigid body movement.



### 3 TRANSFER TO REAL DEFORMATION ANALYSES

The findings gained by the simulations are now transferred to real deformation analyses of artificial and natural objects. A concrete water dam has been sampled by a TLS, several test objects have been sampled by a UAV and surface movements in the alpine region due to solifluction have been sampled by a TLS.

#### 3.1 DEFORMATION OF A CONCRETE WATER DAM

The Brucher dam is a concrete gravity dam in Germany. It has a crown length of 200 m, the height above the foundation bottom is 25 m. The dam is arc-shaped with quite a large radius. Hence, it does not include any large edges as the cuboid in the simulation and it has also less curvature than the Gaussian curve. The dam was scanned in March and June 2016 from three different stations using the Leica ScanStation P20. The point clouds were registered within and between both epochs based on signalized targets.

Fig. 6 shows the M3C2 point cloud comparison of the results. While most of the point cloud differences are in the range of  $\pm 2.5$  mm, there is also a region in the middle of the dam with differences between  $-2.5$  mm and  $-8$  mm. No larger areas of systematically distributed positive differences are visible. The small regions of positive differences are due to plants growing on the dam, see Holst et al. (2017a,b).

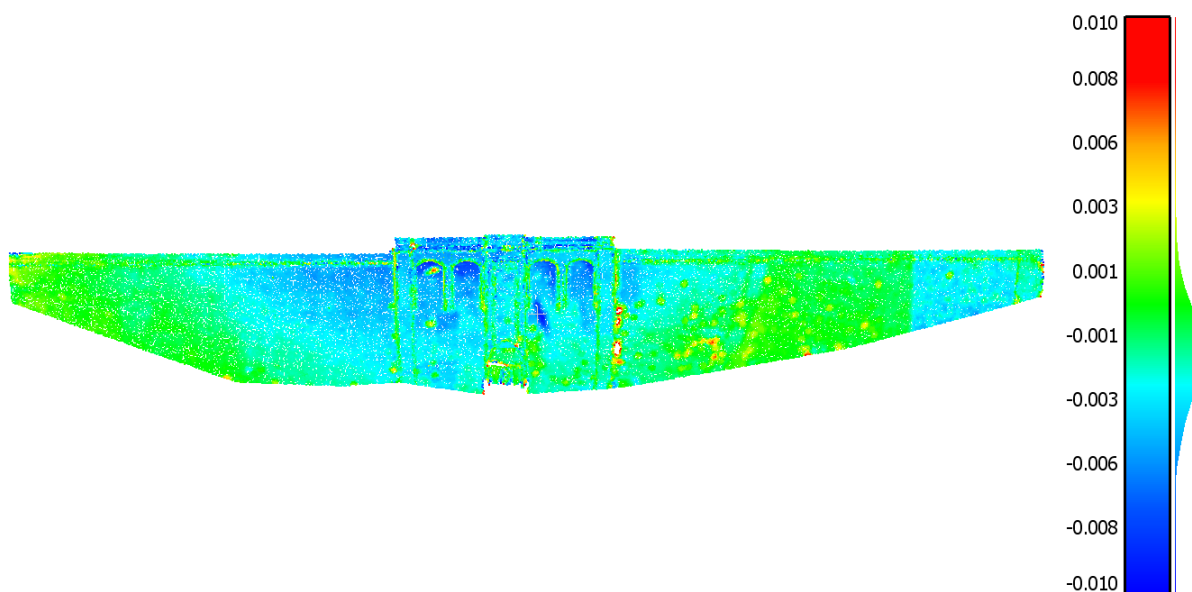


Fig. 6 M3C2 comparison [m] of the Brucher dam at two epochs (CloudCompare)

Based on the interpretations of the previous section, we explain these differences solely by an out-of-plane shape deformation of the dam wall in direction of the water. This result is reasonable since the amount of water stored in the dam was larger in March than in June.

#### 3.2 DEFORMATION OF ARTIFICIAL TEST PIECES

In order to demonstrate the capability of photogrammetry based point clouds to detect deformations, a test field has been set up on an agricultural field, where various objects have been placed and then changed between two measurement epochs. At both epochs, a UAV has been used to take about 300 images (16 Megapixel, Panasonic Lumix GX1, ) from about 20 m

height with an overlap of about 80%. The images have been processed to point clouds using the software Agisoft Photoscan, while the georeferencing was realized using an inhouse developed onboard georeferencing system with an accuracy of about 20 mm (Eling et al. 2015).

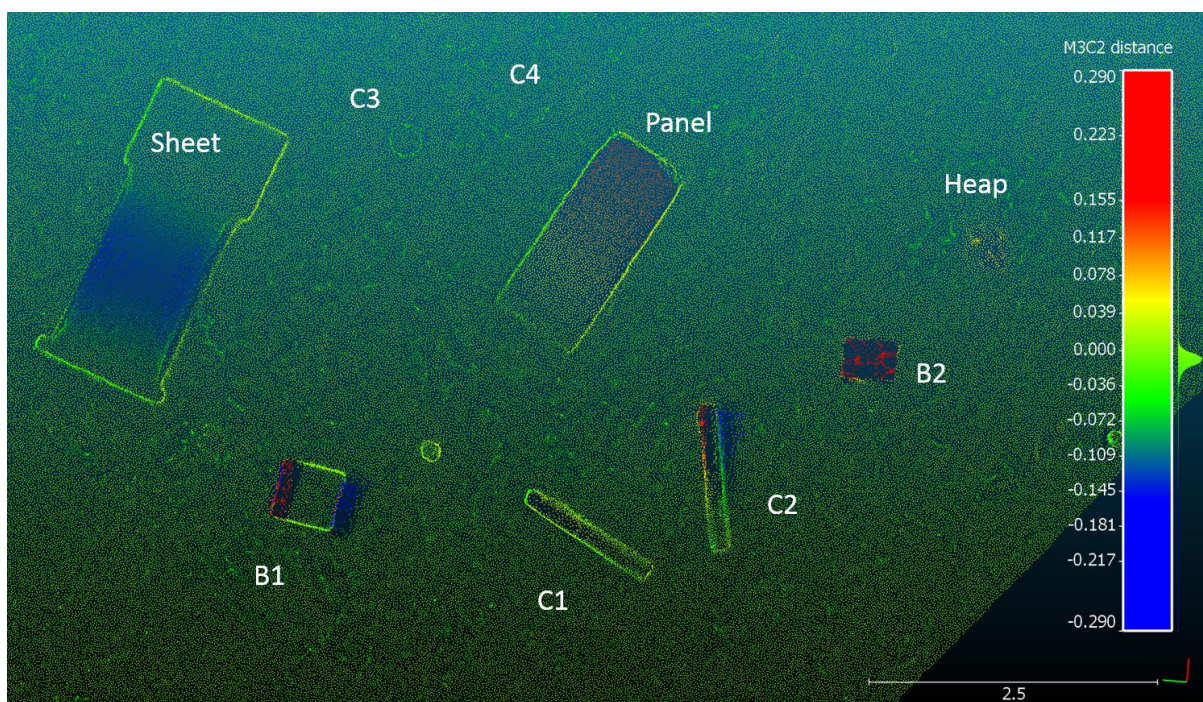
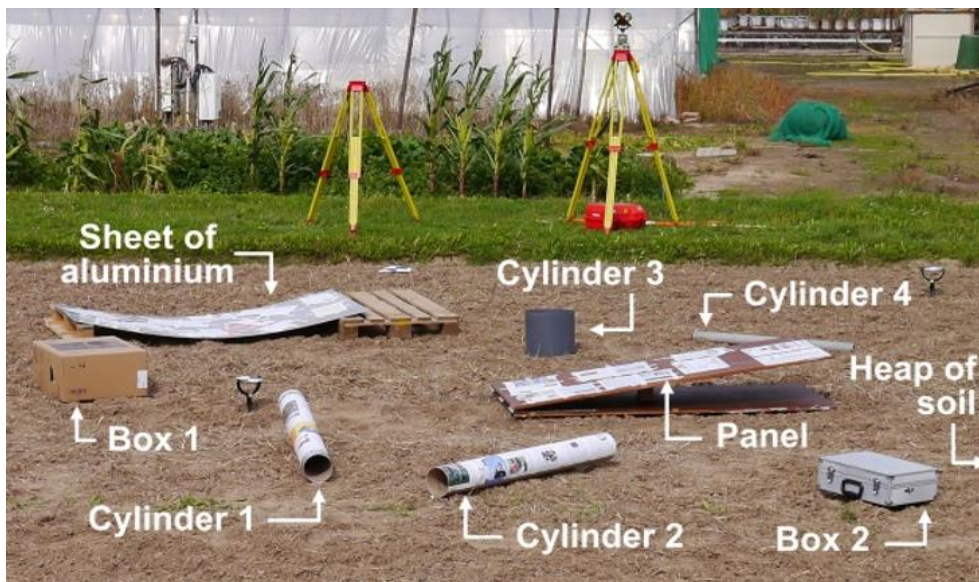


Fig. 7 (Top) Test field; (Bottom) M3C2 comparison of test filed at two epochs (CloudCompare). Between the epochs certain deformations have been applied intentionally.

The difference between the point clouds at both epochs are again calculated using the M3C2 algorithm. The aluminium sheet was lowered about 10 cm in the middle. Box 1 was moved about 10 cm towards the left. The angle between the panel and the ground was increased about 5 degrees. Cylinder 1 was rotated 5 degrees around the horizontal axis, cylinder 2 5 degrees around the vertical axis. Box 2 was added at the second epoch and a heap of soil with



about 10 cm height was created next to Box 2. Cylinder 4 was not moved, cylinder 3 was moved about 10 cm. Similar to the results from the simulations, the deformations are visible as a pattern in the colour scheme, but the exact type of deformation cannot always be inferred without any prior knowledge about the object and the deformation. The bending of the sheet and the inclinations of the panel and cylinder 1, as well as the addition of box 2 and the heap of soil are clearly visible and easy to interpret as they are out of plane changes of the scene. In plane motions of objects (B1, C2) show the same pattern as described in Section 2.1. Cylinder 3 is not visible at all, due to its geometry. Within the photogrammetric processing of the images thin vertical structures may be considered as noise and therefore not reconstructed. Despite this disadvantage compared to laserscanning, the experiment shows that also image based point clouds can be used to detect certain deformation types.

### 3.3 MOVEMENT DUE TO SOLIFLUCTION

Solifluction is the slow downslope movement of soil mass resulting from freeze–thaw processes, which occurs on hillslopes in Polar and Alpine regions (Eichel et al. 2016). Solifluction appears in the form of lobes. These lobes contain a lobe head that builds the front part moving down the surface. These heads are curved, their height varies between about 0.2 m and 0.5 m in the present study region. The tail of the lobe is shaped smooth and transists in the surrounded not moving surface. Hence, the form is a combination of the two objects simulated in section 2.

The corresponding study region of a size of 200 m x 120 m was sampled in September 2014 and September 2016 by the TLS Leica ScanStation P20. About 15 stations were set up in both epochs to acquire a scan point spacing of several centimetres. For a stable geodetic datum, 5 ground points were marked in the solid rock.

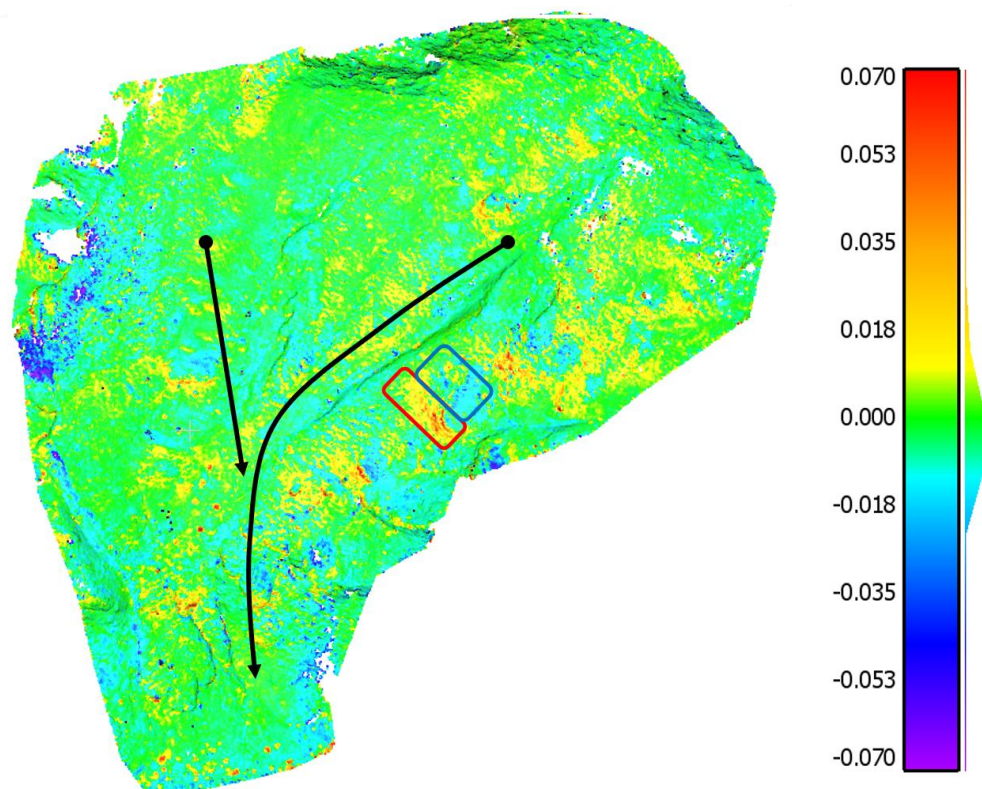


*Fig. 8 M3C2 comparison [m] of the alpine study region (CloudCompare) with downhill direction (black arrows)*



Fig. 8 shows the resulting M3C2 comparison leading to three observations: (1) most of the differences are in the interval of  $\pm 8$  mm. (2) Only at several positions, sharp anomalies of more than  $+50$  mm occur (e.g., Fig. 8, red box). (3) These are followed most times by larger sections of negative differences smaller than  $-30$  mm (e.g., Fig. 8, blue box). Following section 2, observation (2) seems to represent the in-plane movement of the lobes at their heads. Since the lobes are highly curved at this position, these differences of larger than  $+50$  mm do not necessarily represent the true movement, cf. section 2. Observation (3) implies that the solifluction also leads to an out-of-plane shape deformation. If this was not the case, the difference patterns would look more similar to the ones of Fig. 4. Both observations have to be analysed further in a prospective study. Finally, observation (1) does only imply that no out-of-plane movement exists in the present study region. However, it cannot be stated whether the surfaces moves in-plane, i.e., it flows or not.

## 4 CONCLUSION

In many applications, point cloud comparisons, i.e., the M2M or M3C2 comparison, are used for revealing deformations. While these point cloud comparison are easy to process due to several software packages, their interpretation can be difficult: dependent on the type of deformation – rigid body movement or shape deformation – and dependent on the direction of deformation – in-plane or out-of-plane, the interpretation can lead to false results. Furthermore, the geometry of the acquired object, i.e., its curvature, leads to the fact that similar types and directions of deformation might appear differently in a point cloud comparison. This has been shown in the present study for simulated and real examples.

In consequence, point cloud comparisons should not be used without prior knowledge about the observed object's geometry. Instead, it should always be thought about (1) the potential deformations that may act on an object and also (2) what pattern these potential deformations produce in a point cloud comparison. Only then, it can, e.g., be specified whether the quantity of the point cloud differences (as is the case at out-of-plane deformations) or rather the size of the region showing this quantity (as might be the case at in-plane rigid body movements of highly curved objects) is the relevant parameter for revealing the deformation.

## REFERENCES

- Barnhart, T.B., Crosby, B.T. (2013): Comparing two methods of surface change detection on an evolving thermokarst using high-temporal-frequency terrestrial laser scanning, Selawik River, Alaska. *Remote Sensing*, 5(6), 2813-2837
- Eichel, J., Draebing, D., Klingbeil, L., Wieland, M., Eling, C., Schmidtlein, S., Kuhlmann, H. & R. Dikau (2017): Solifluction meets vegetation: the role of biogeomorphic feedbacks for turf-banked solifluction lobe development. *Earth Surface Processes and Landforms*. DOI: 10.1002/esp.4102
- Eling, C., M. Wieland, C. Hess, L. Klingbeil, H. Kuhlmann (2015). Development and evaluation of a UAV based mapping system for remote sensing and surveying applications. In: Proc of the UAV-g conference. *International Archives of the Photogrammetry, Remote Sensing and Spatial Information Sciences*, Vol. XL-1/W4, pp. 233-239

- Heunecke, O., Kuhlmann, H., Welsch, W., Eichhorn, A., Neuner, H. (2013): Handbuch Ingenieurgeodäsie. Auswertung geodätischer Überwachungsmessungen. 2. Edition, Wichmann, Heidelberg
- Holst, C., Kuhlmann, H. (2016): Challenges and present fields of action at laser scanner based deformation analyses, *J. Appl. Geodesy*, 10 (1), 17-25
- Holst, C., Schmitz, B., Schraven, A., Kuhlmann, H. (2017a): Eignen sich in Standardsoftware implementierte Punktwolkenvergleiche zur flächenhaften Deformationsanalyse von Bauwerken? Eine Fallstudie anhand von Laserscans einer Holzplatte und einer Stauwand, *Zeitschrift für Vermessungswesen zfv*, 2/2017
- Holst, C., Schmitz, B., Kuhlmann, H. (2017b): Investigating the applicability of standard software packages for laser scanner based deformation analyses, *FIG Working Week 2017*, 29 Mai – 2 June, Helsinki, Finland
- Mukupa, W., Roberts, G.W., Hancock, C.M., Al-Manasir, K. (2016): A review of the use of terrestrial laser scanning application for change detection and deformation monitoring of structures, *Survey Review*
- Neuner, H., Holst, C., Kuhlmann, H. (2016): Overview on current modelling strategies of point clouds for deformation analysis, *Allgem. Verm. Nachr.*, 11/2016, Wichmann Verlag, Berlin
- Ohlmann-Lauber, J., Schäfer, T. (2011): Ansätze zur Ableitung von Deformationen aus TLS-Daten. Schriftenreihe DVW, Band 66 „Terrestrisches Laserscanning - TLS 2011 mit TLS-Challenge“, 147-157, Wißner Verlag
- Wunderlich, T., Niemeier, W., Wujanz, D., Holst, C., Neitzel, F., Kuhlmann, H. (2016): Areal deformation analysis from TLS point clouds – the challenge. *Allgem. Verm. Nachr.*, 11/2016, Wichmann Verlag, Berlin